Spring 5-10-2009

Contribution of the Novel C-terminal Domain to the Ribosome Binding Activities of Virulence Regulator BipA

Heeren Makanji
University of Connecticut - Storrs, heeren.makanji@gmail.com

Contribution of the Novel C-terminal Domain to the Ribosome Binding Activities of Virulence Regulator BipA

Heeren Makanji

May 1, 2009

University of Connecticut

University Scholars/Honors Program

Major Advisor: Dr. Victoria Robinson

Associate Advisor: Dr. Debra Kendall

Associate Advisor: Dr. David Knecht

Abstract

Contribution of the Novel C-terminal Domain to the Ribosome Binding Activities of Virulence Regulator BipA

Heeren Makanji, University Scholars Program

University of Connecticut
2009

Bacterial GTPases regulate many cell functions, including the stress response, signal recognition, protein synthesis, and cell differentiation, through a molecular switch that is activated and deactivated depending on their nucleotide bound state (1). A member of the translational family of bacterial GTPases along with LepA and EF-G, BipA is a 67 kD protein that is essential for virulence and the stress response. Crystal structures from the Robinson lab have shown a unique C-terminal domain on BipA that has been implicated in ribosome binding. Using N-terminal deletion constructs, we have shown that the C-terminal domain is necessary, but not sufficient, to promote interaction of BipA with the ribosome. We have also identified key structural elements within the CTD that are required for ribosome association and have investigated amino acid residues within those elements. Because BipA exerts it function through interactions with the ribosome, these data serve as a preliminary step to elucidating BipA's role in the cell.

Acknowledgements

There were several people who were integral to my involvement in research and the successful completion of my University Scholar project.

I would like to thank Dr. Victoria Robinson, without whose patience, guidance, and enthusiasm, I would not have developed my interest in research. Her commitment to my development gave me the flexibility to work towards completing this project and exploring other areas that interested me.

I also want to thank Dr. Megan deLivron, who sacrificed the time and put forth the effort to train me in the lab. Her patience, especially when things did not work correctly, helped me develop my confidence. Meg was also instrumental in making the lab atmosphere friendly and enjoyable

I would like to thank the other members of the Robinson group: Robbins, Chifei, Maura, and Raj. Their humor and friendly demeanor made the lab a second home.

I also want to thank Dr. Debra Kendall, whose guidance, both in the sciences and in life, has helped me reach many of my goals.

I would like to thank Dr. David Knecht for being a member of my committee and giving me advice every step of the journey.

I also want to thank the University of Connecticut Honors Program for their perennial support of my research endeavors. Through the SURF, Life Sciences Honors Thesis Grant, and OUR grant, they helped make many research ideas a reality.

Table of Contents

List of Figures

List of Tables

Introduction

I. GTPases

Bacterial GTPases regulate many cell functions, including the stress response, signal recognition, protein synthesis, and cell differentiation (1). All GTPases contain a universally conserved G-domain that is involved in the basic functions of GTP binding and hydrolysis. This domain consists of a six-stranded mixed β-sheet surrounded by five alpha helices (2). Within the G domain are five consensus sequences that are involved in the proper arranging of the nucleotide in the binding pocket. The first of these stretches, called the G1 (GXXXXGKT/S) motif, forms the P loop (phosphate binding loop), which interacts with the β and γ phosphates on the nucleotide. The G2 (XXTX) and G3 (DTXG) motifs also interact with these phosphate groups (Figure 1). The G4 (NKXD) and G5 (SAK) motifs are involved in recognition of guanosine (2).

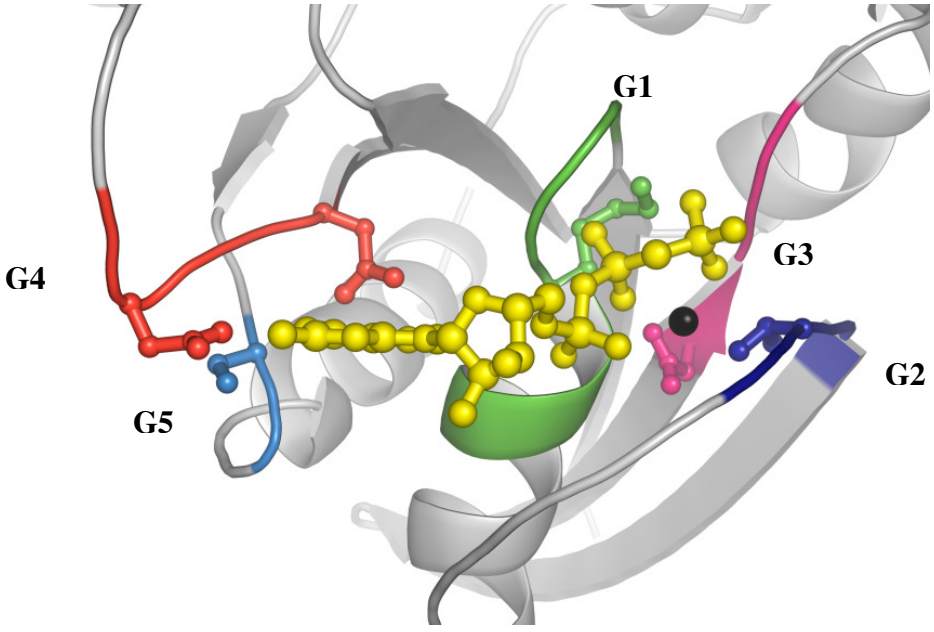

Figure 1. **The typical GTPase nucleotide binding pocket.** A ribbon diagram of the nucleotide binding site of the GTPase Ras. The G1 (green), G2 (blue) and G3 (pink) motifs contact the β and γ phosphates of the nucleotide. The G4 (red) and G5 (aqua) motifs contact the guanosine of the nucleotide (Image courtesy of Dr. Victoria Robinson).

In addition to these common structural features, GTPases are also united by a common mechanistic theme, molecular switching through conformational change. In the majority of GTPase families, the protein becomes "activated" for its particular function upon binding GTP. As soon as GTP is hydrolyzed to a GDP, the protein becomes "inactive" and eventually sheds the GDP to return to an empty state, ready to remain off or turn on according to cellular needs (2). Guanine nucleotide binding and release promotes structural rearrangement in the Switch I and Switch II regions of the G domain. This,in turn, alters the surface properties of the protein, making the switch regions "hot spots" for binding and/or effector properties (Figure 2). The mechanism for structural change resembles a loaded spring with the γ phosphate serving as the hook (3). When GTP is hydrolyzed and the phosphate is released, amino acid residues that once interacted with the phosphate lose those connections and the switch regions move into a relaxed, unloaded conformation

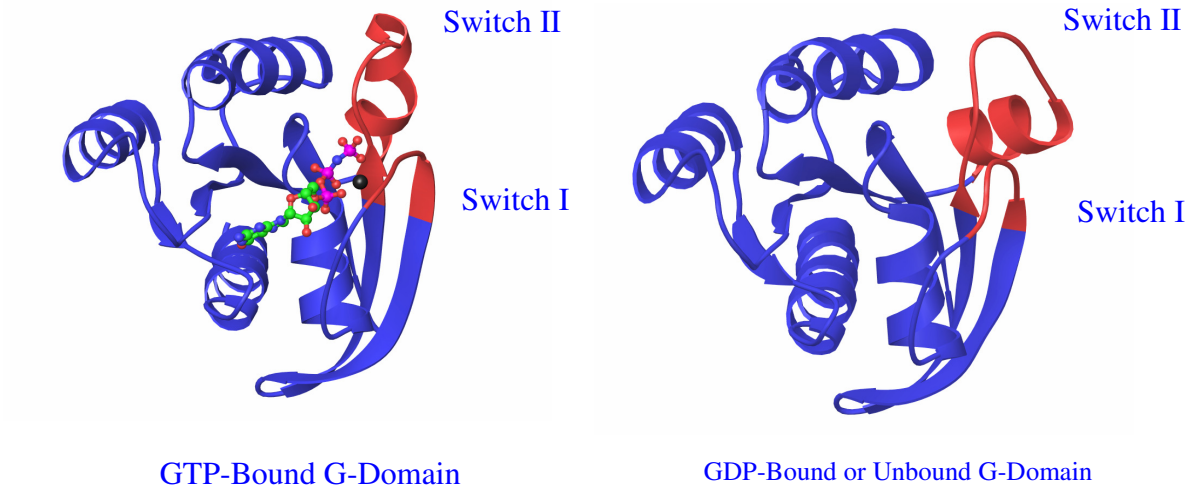

Figure 2. **The conformational changes in the switch regions of the G domain**. A ribbon diagram of the Ras G-domain. In the GTP-bound state, the γ phosphate interacts with residues in the switch regions to create a tighter conformation. In the GDP-bound and unbound state, these contacts are lost and the switch regions change conformationally and relax. (Image courtesy of Dr. Victoria Robinson)

In the Robinson lab, the focus of our research is to investigate bacterial GTPases. There are dozens of well-characterized bacterial GTPase families, all of which have been shown to bind the ribosome to exert their function in the cell. We are particularly interested in a member of the translational family of GTPases, BipA. BipA is conserved across many pathogenic bacterial species and its interaction with the ribosome presents an ideal aim for antimicrobial research. Antibiotics exert their inhibitory action in many ways, including competing with substrates, altering ribosomal dynamics, limiting ribosomal flexibility, promoting improper coding, and blocking the tunnel in the large subunit that is used by the nascent polypeptide (4). Nevertheless, new targets, especially those are accessible across a wide spectrum bacterial species, are necessary to keep an advantage in the battle against microbes. While we do not understand BipA's function in the cell, its phenotypic effects show that the protein is involved in stress control and virulence. From comparison with other members of the translational family, it is likely that the novel C-terminal domain of BipA is essential to its function. Through investigation of this domain, this thesis hopes to uncover key regions of the CTD essential to BipA function

II. The Ribosome

Oneof the most complex macromolecular machines in a cell, the ribosome is involved in translating messenger RNA into polypeptide chains. The bacterial 70S ribosome is made up of a large 50S subunit and a small 30S subunit, both of which consist of rRNAs and proteins. The 50S subunit contains a 5S rRNA, 23S rRNA, and thirty-three proteins while the 30S subunit consists of 16S rRNA and twenty-one proteins

(5). Before translation beings, the two subunits are found as separate species, and the proper binding of mRNA to the 30S subunit serves as the initiation step to bring the subunits together.

The process of translation is extremely complex, but I have offered a simplified version in this thesis (5). After an aminoacyl-transfer RNA molecule with formylmethionine recognizes the AUG initiation codon, each codon thereafter enters the aminoacyl binding site, allowing the appropriate aminoacyl-transfer RNA molecule to bind. After addition of an amino acid to the growing chain at the aminoacyl site, EF-G catalyzes the translocation of the uncharged transfer RNA molecule from the peptidyl binding site to the exit site and the peptidyl-transfer RNA molecule from the aminoacyl binding site to the peptidyl binding site. When a new aminoacyl-transfer RNA molecule enters the aminoacyl site, the uncharged transfer RNA molecule is expelled from the exit site, renewing the cycle, which will continue until a stop codon is encountered. The nascent polypeptide, which is often several hundred amino acids in length, grows through a tunnel located in the large subunit that provides an environment free of proteases and suitable for the early stages of folding (5). A space-filling diagram showing the cellular elements involved in translation is shown in figure 3.

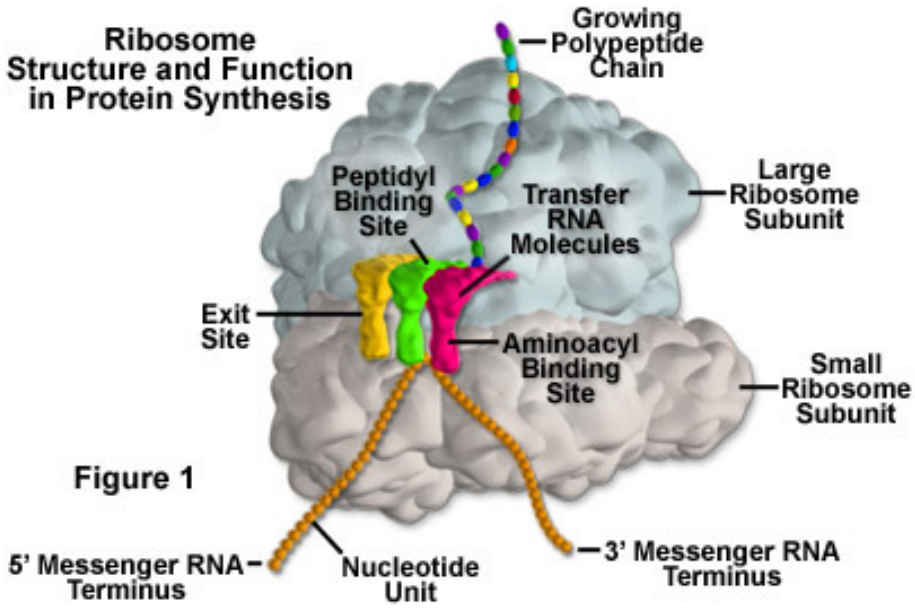

Figure 3. **The ribosome and messenger RNA translation.** A space-filling diagram showing the ribosome and elements involved in translation. The messenger RNA chain is shown binding to the aminoacyl site of the ribosome, where the correct aminoacyl-transfer RNA molecule (red) with the complementary anti-codon will also bind. The peptidyl-transfer RNA molecule (green) is shown in the peptidyl binding site with the nascent, growing polypeptide chain exiting through a tunnel in the large subunit. (Adapted from Dr. Michael Davidson, Florida State University (6))

III. The Cellular Properties of BipA

In 1995, Qi et al. reported that bactericidal/permeability-increasing protein (BPI), a cationic antimicrobial protein from neutrophils, induced a sevenfold increase in the expression of a novel protein (7). This protein, named BipA, belonged to the GTPase family and shared sequence homology with the translation factor EF-G. Many research groups have since characterized phenotypes of *Salmonella typhimurium* and *Escherichia coli* deletion strains (8). BipA has been shown to be a tyrosine-phosphorylated GTPase involved in interactions between epithelial cells and enteropathogenic E*scherichia coli* (8). Mutants lacking BipA adhere to epithelial cells in culture, but are unable to induce a

cytoskeletal rearrangement in the cells that is characteristic of hosts infected by wild-type strains. Conversely, increased expression of BipA leads to increased remodeling of actin elements. BipA was also observed to control flagella-mediated cell motility and resistance to the antibacterial effects of a human defense protein. In 2003, Grant et al. reported BipA is involved in regulation of several cell-surface and virulence-associated components in enteropathogenic *E. coli* (9). Bacterial flagella, the *espC* pathogenicity, and a type III secretion system were a few of the components controlled by BipA.

In 2008, deLivron et al. showed that BipA has two distinct ribosome binding modes. BipA binds the 70S ribosome in the GTP-bound state during normal growth conditions but binds the 30S small subunit under stress conditions (10). The researchers have implicated the alarmone ppGpp as being involved in the differential association of BipA with ribosomal species.

While all initial characterizations of BipA focused around pathogenicity, the Flowers group were first to report that BipA serves a regulatory role and is necessary for growth of *E. coli* K12 in cold temperatures (11). The finding was unexpected, as the group realized that one of its lab strains, D10, had become cold-sensitive, and they genetically analyzed the bacteria to reveal a disruption in the BipA gene. Interestingly, the BipA from *E. coli* K12 is not phosphorylated, showing that BipA has regulatory roles that are independent of phosphorylation.

The Flowers group later reported that insertion mutations in the gene for rluC were able to suppress the cold-sensitive phenotype of ΔBipA (12). The rluC gene codes for a pseudo-uridine synthase that modifies 23S rRNA at three sites near the peptidyl transferase center. Because the deletion of rluC suppressed cold sensitivity, the group

suggested, just as Qi et al. previously had, that the phenotypic effects of BipA are a result of an interaction with the ribosome. It was also suggested that BipA has a role in the structure or function of the ribosome and that a lack of pseudo-uridylation at the three sites on the ribosome made the ribosomes BipA-independent.

IV. Structural Features of BipA, LepA, and EF-G

As mentioned previously, amino acid sequence analysis indicates BipA is a member of the translational GTPase family. Members of this GTPase family are involved with regulating some aspect of the translation process. Among this group's members are EF-G and LepA, which share significant sequence homology with BipA. EF-G is a well-studied ribosomal factor that catalyzes translocation during polypeptide formation (13). Recently, LepA has been characterized as a translation factor that aids in accurate protein synthesis by inducing backwards translocation after defective forward reactions (14). BipA's function in the cell is unknown, but a characterization of its structural features, especially its C-terminal domain, will help elucidate the relationship between BipA and the ribosome. According to the crystal structure of *Salmonella enterica* BipA obtained from the Robinson Lab, the protein contains five distinct domains (Figure 4). The N-terminal G-domain (red) is followed by a β-barrel domain II. Domains III and IV are α/β domains. Domain V, the C-terminal domain, contains a novel fold that has been shown to be essential to ribosome binding.

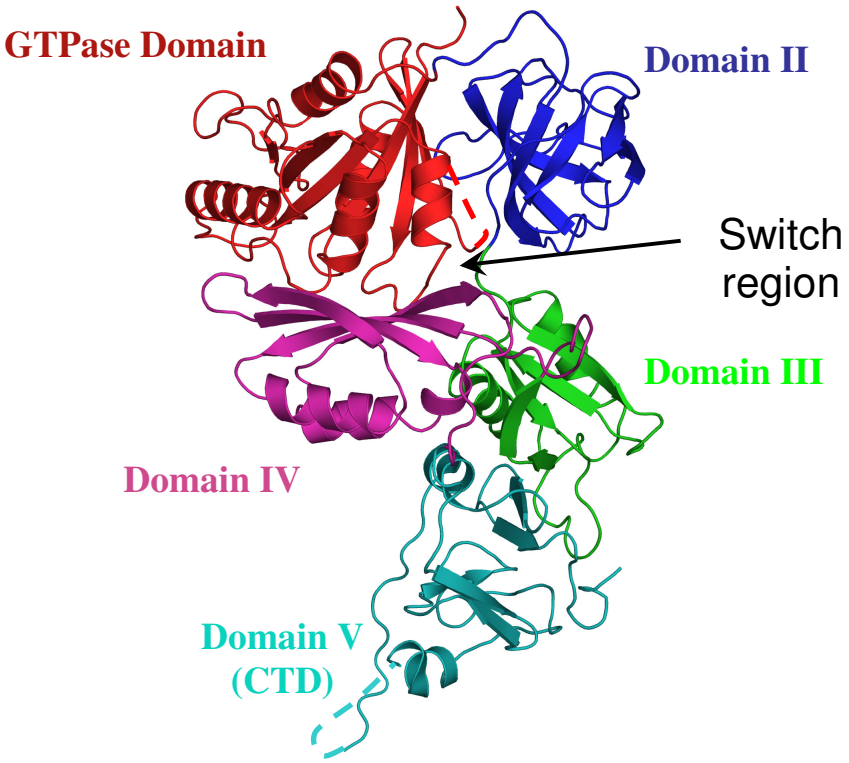

Figure 4. **Crystal structure of BipA.** A ribbon diagram of the GTPase BipA depicting the five domains of the protein. Domain I (red) is the G domain, Domain II (blue) is a β-barrel and Domains III (green) and IV (magenta) are α/β domains. The novel C-terminal domain (light blue) has been implicated as a determinant of protein function (Image courtesy of Dr. Victoria Robinson).

A comparison of the structural features of BipA, LepA (PDB 3CB4, 15), and EF-G (PDB 1N0U, 16) is shown in figure 5. The domains in each of these proteins haven been labeled I through V starting at the N-terminus. Domains I, II, and III are topologically equivalent in all three proteins with the exception that EF-G contains a G' domain, which is not universally conserved in G proteins. Domain IV in EF-G is positioned at the distal end opposite the G domain, while Domain IV in BipA and LepA is located adjacent to the G domain; the only similarity in these domains is their numbering. Domain V of EF-G and domain IV of BipA and LepA are equivalently positioned and contain significant similarity in their structure.

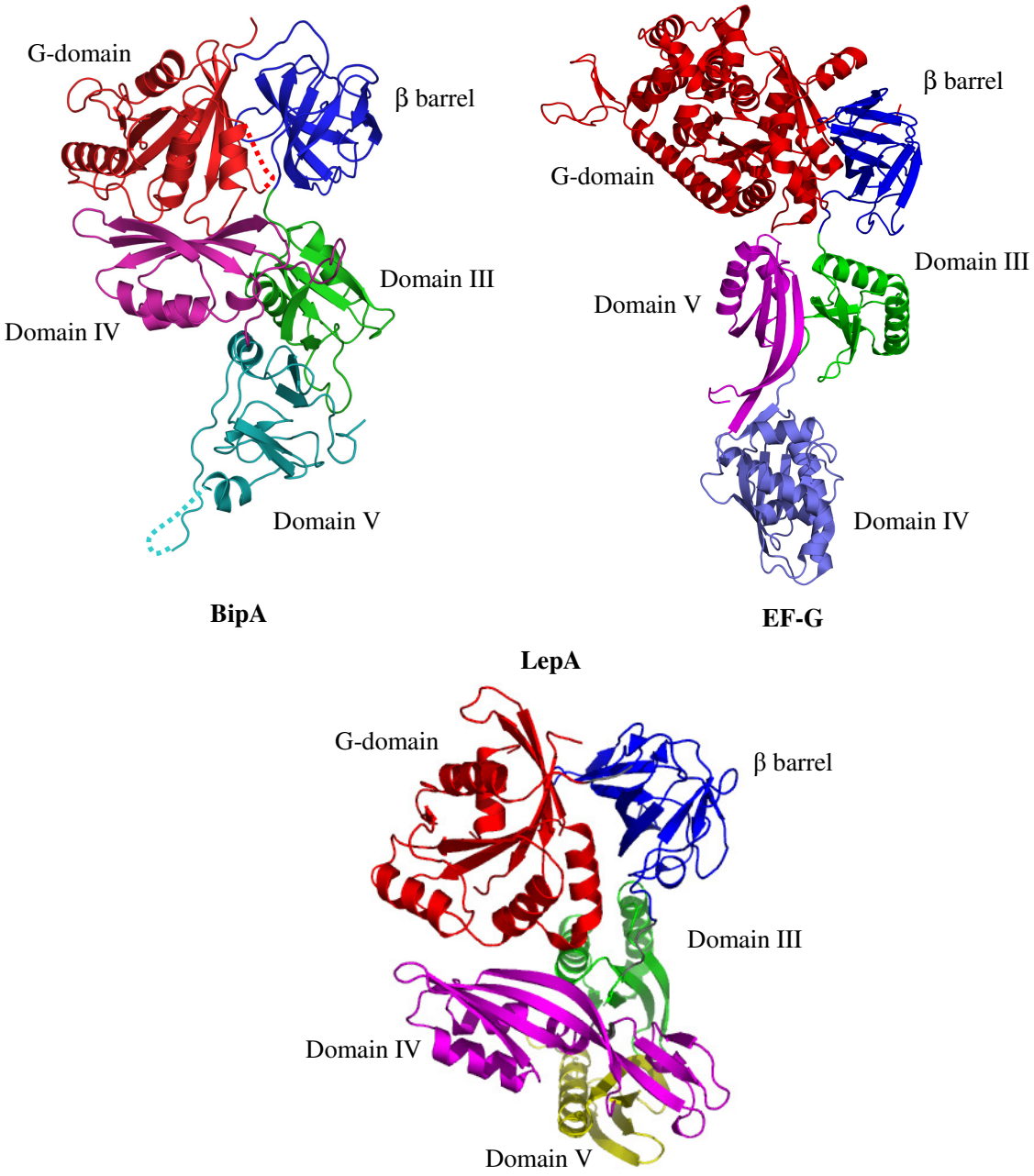

Figure 5. **Comparison of BipA, LepA, and EF-G structures.** Ribbon diagrams of BipA, LepA (PDB 3CB4, 15) , and EF-G (PDB 1N0U, 16). BipA, LepA, and EF-G contain structurally equivalent domains I, II, and III. Domain IV in BipA and LepA and Domain V in EF-G occupy equivalent positions and have similar structure. The C-terminal domain of all three G proteins is the distinctive structural feature (BipA image courtesy of Dr. Victoria Robinson).

Unlike the rest of the protein, the C-terminal domains of BipA and LepA and domain IV of EF-G are discrete. In BipA, this domain is extremely unstructured and flexible, as suggested by the inability to resolve some of its configuration. The CTD contains both α-helices and β-sheets as well as many loop regions that contribute to its flexible nature. In fact, both LepA and EF-G also contain α-helices and β-sheets, but the frequency and positions of these secondary structural elements is unique in all three proteins (Figure 6).

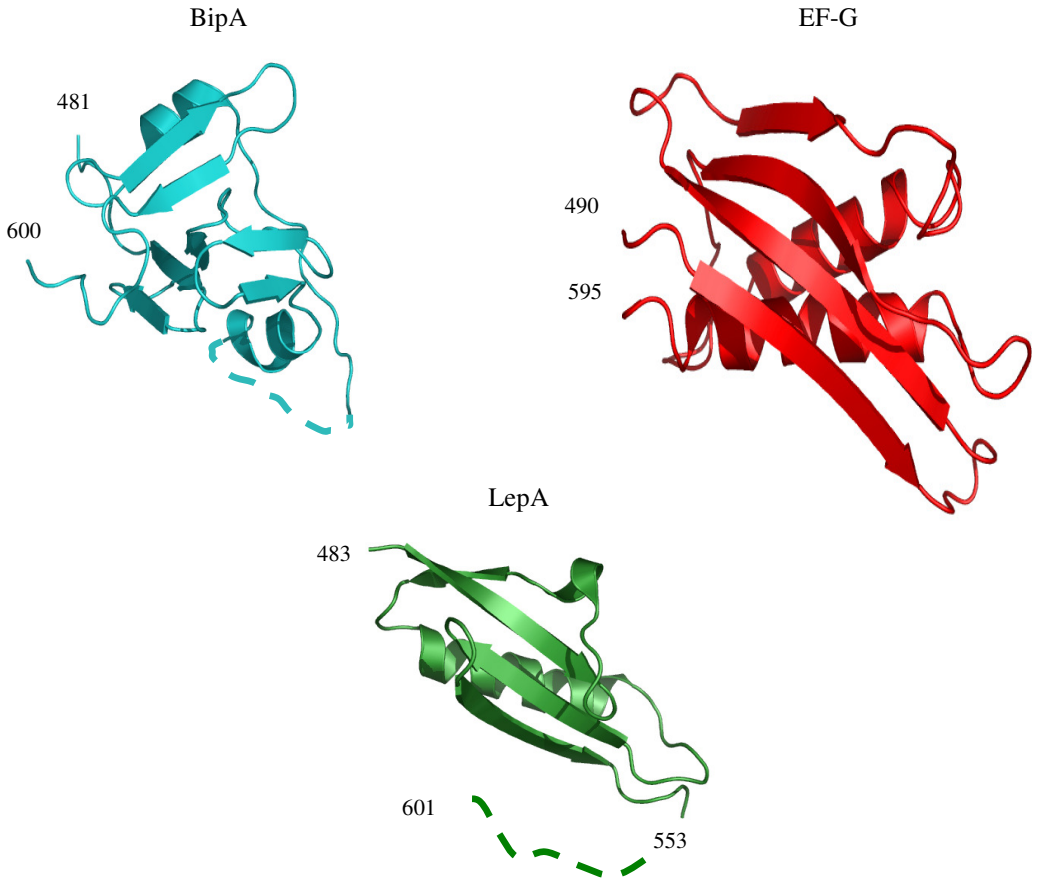

Figure 6. **Comparison of BipA and LepA domain V and EF-G domain IV.** Ribbon diagrams of BipA and LepA domain V and EF-G domain IV. The domain in each protein that sits distal to the G domain is shown above. All three domains have a combination of α-helices, β-sheets and long loop regions (Images courtesy of Dr. Victoria Robinson).

Because they are designated as members of the same family of proteins, it follows that BipA, LepA, and EF-G would have structural similarity (as they clearly do). But within this family, we suggest that their distinct functions are a direct result of the distinct domain that sits distal to the G domain (domain IV in EF-G and domain V is BipA and LepA, figure 7).

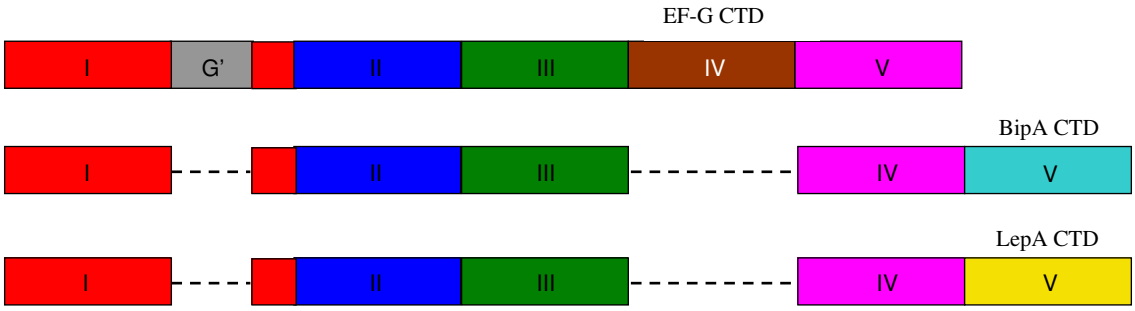

Figure 7. **Schematic representation of domain architecture in BipA, LepA, and EF-G.** A domain-wise depiction of BipA, LepA, and EF-G. The domains colored red, blue, green, and magenta are equivalent in all three G proteins. Distinct to each protein is domain IV in EF-G and domain V in BipA and LepA (Image courtesy of Dr. Victoria Robinson).

While the cellular function of BipA remains unknown, it has been shown that this translational GTPase binds the 70S ribosome. We hypothesize that BipA exerts its function by binding the ribosome, similar to the other members of the protein family. Therefore, we have attempted to map the 70S ribosome binding surface on BipA, with an emphasis on the novel C-terminal domain that has been shown to be essential to binding.

V. Preliminary Studies

A series of experiments were used in the Robinson lab to uncover the role of the C-terminal domain in BipA (deLivron and Robinson, to be published). The BipA gene was

inserted into a plasmid and truncation constructs were selectively amplified using PCR (Figure 8).

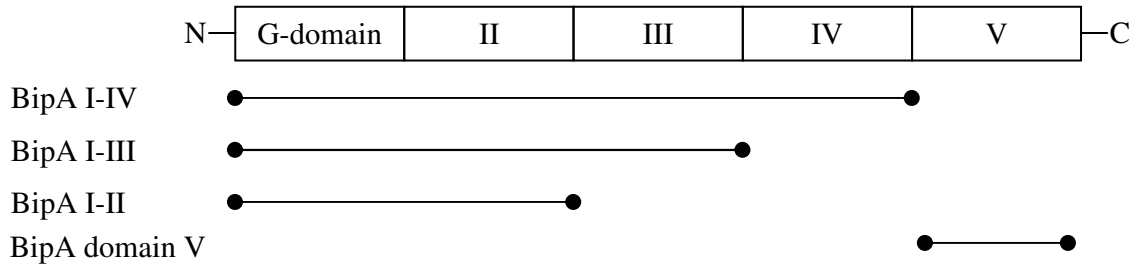

Figure 8. **Truncation constructs of BipA.** Schematic depiction of the truncation constructs of BipA. Truncation constructs were made to investigate the ribosome binding properties of the C-terminal domain. These truncations were amplified from the BipA gene inserted on a plasmid and then assayed for ribosome binding *in vivo* (Image courtesy of Dr. Victoria).

The data showed that BipA I-II, BipA I-III, and BipA I-IV were unable to bind the 70S ribosome, while the full-length BipA bound the 70S ribosome *in vivo*. This observation led to the creation of a BipA domain V construct, but it was unable to bind the ribosome. The following studies were designed to identify the ribosome binding surface of *S. enterica* BipA.

.

Materials and Methods

I. Deletion Constructs and Site-Directed Mutagenesis

All deletion constructs and site-directed substitutions were created using specially designed primers from IDT DNA. Primers were designed for site-directed mutagenesis as outlined by Zheng et al (17). Basic parameters followed for primer design include a primer length between 25 and 45 base pairs, melting temperatures of less than 80°C, similar melting temperatures for both the forward and reverse primer, at least 10 correct base pairs flanking each side of a single base pair mutation and 15 correct base pairs flanking each side of a double base pair mutation, GC content near 50%, and at least a 10 base pair differences in the forward and reverse primers (to minimize self-annealing). These represent ideal conditions, but the actual primer design is limited by the DNA sequence being manipulated. Primers used to create the truncation constructs and site-directed substitutions are shown in Table 1.

Table 1

S. enterica BipA Construct	***Primers***
III-IV (306-607)	5’-ctaacgt**CATATG**accgtgtctatgttcttctgcgt-3’ (Forward)
	5’-cgt**CTCGAG**ttactcttctttctgaccacggttcgc-3’ (Reverse)
BipA (1-596)	5’-ctaacgta**CATATG**gtgatcgaaaatttgcgtaacatcgcc-3’
	5’-cgt**CTCGAG**ttaatcgttttccgtcaggtgacg-3’
R422A/K423A	5’-cgctgggcgag**GCTGCA**ggcgacctgaaaaacatgaat-3’
	5’-ttcaggtcgcc**TGCAGC**ctcgcccagcgcctgcatga-3’
K434A/R436A	5’-catgaatccggacggt**GCC**ggc**CCG**gtacgtctcgac-3’
	5’-cacgtagtcgagacgtac**GGC**gcc**TGC**accgtcc-3’
R507A	5’-cggtttgcaggat**GCC**ggtaagctgttcctgg-3’
	5’-gaacagcttacc**GGC**atcctgcaaaccgaaca-3’
K509A	5’-gtttgcaggatcgcggt**GCT**ctgttcctgggtcac-3’
	5’-ccgtgacccaggaacag**AGC**accgcgatcctgcaa-3’
R507/K509A	5’-gcgcggcactgggtcctgtctcgt**GGC**cgtaggacg-3’
	5’-cgcgccgtgacccaggaacagagca**CCG**gcatcctg-3’
H514A	5’-tgttcctgggt**GCC**ggcgcggaagtttatgaag-3’
	5’-cttccgcgcc**GGC**acccaggaacagcttaccgc-3’
H527A	5’-gtttatgaaggccagattattggtatt**GCC**agtcgctcca-3’
	5’-cgtcaggtcgttggagcgact**GGC**aataccaata-3’
H514A/H527A*	5’-gtttatgaaggccagattattggtatt**GCC**agtcgctcca-3’
	5’-cgtcaggtcgttggagcgact**GGC**aataccaata-3’
H527K	5’-aggccagattattggtatt**AAG**agtcgctccaacgacc-3’
	5’-tcaggcgttggagcgact**CTT**aataccaatasatctgg-3’
D532A	5’-acagtcgctccaac**GCC**ctgagcgtaaac-3’
	5’-cagtttaccgtcag**GGC**gttggagcgact-3’
D552A	5’-cgtctggtacg**GCT**gaagcggtgattctg-3’
	5’-atcaccgcttc**AGC**cgtaccagacgcacg-3’
D532A/D552A*	5’-cgtctggtacg**GCT**gaagcggtgattctg-3’
	5’-atcaccgtttc**AGC**cgtaccagacgcacg-3’
K562A	5’-ggttccgccaatt**GCA**atgagccttgagcaagcg-3’
	5’-ctcaaggctcat**TGC**aattggcggaaccagaatc-3’
R588A	5’-aggcagtccactgcaaa**TCG**ctatgcctatctccagc-3’
	5’-caatgaactc**CGC**cgcttgctcagcgctca-3’

Table 1. **Primers used for deletion constructs and site-directed substitutions**. A list of the primers designed for polymerase chain reaction (PCR). The construct or substitution is shown in the left column and its corresponding forward primer (top) and reverse primer (bottom) are shown on the right. The capitalized and bolded sequences code for the restriction site (for constructs) or amino acid (for substitutions) that has been introduced. *The H514A/H527A and D532A/D552A substitutions were completed by introducing the second substitution into a pET28a plasmid containing the first substitution.

The N and C-terminal deletion constructs were created by polymerase chain reaction (PCR) from *Salmonella enterica* genomic DNA (ATCC 700720D). This PCR cycle amplified the entire BipA gene and introduced *Nde*1 and *Xho*1 cut sites at appropriate regions to create the constructs of interest, BipA III-V (containing residues 306-607) and BipA (1-596). The resulting cDNA was incubated with Nde1 and Xho1 for 1 hour at 37°C and purified using plasmid purification kit. The cleaned product was then incubated with cut pET28a template and T4 DNA Ligase overnight. *E. coli* DH5α cells were transformed with the ligation mixture using heat shock and plated on kanamyacin plates to select for transformed colonies. Ten colonies were analyzed by colony PCR and DNA gel electrophoresis to check for appropriately sized insert. Plasmids were confirmed by sequencing at the DNA Biotechnology Center, University of Connecticut.

Site-directed substitutions were generated by PCR using pWW3 as a template. The PCR mixture was incubated with Dpn1 at 37°C for 1 hour to eliminate template, methylated DNA that did not contain the mutation. The plasmid was isolated using a plasmid purification kit and subsequently used to transform DH5α cells with heat shock and plated on kanamyacin plates. A single colony was taken from the plate to inoculate an overnight culture grown at 37°C. Copies of pET28a were isolated from the culture using a plasmid purification kit and presence of plasmid confirmed using DNA gel electrophoresis (Figure 9). The presence of the base pair mutations was confirmed by sequencing at the DNA Biotechnology Center, University of Connecticut.

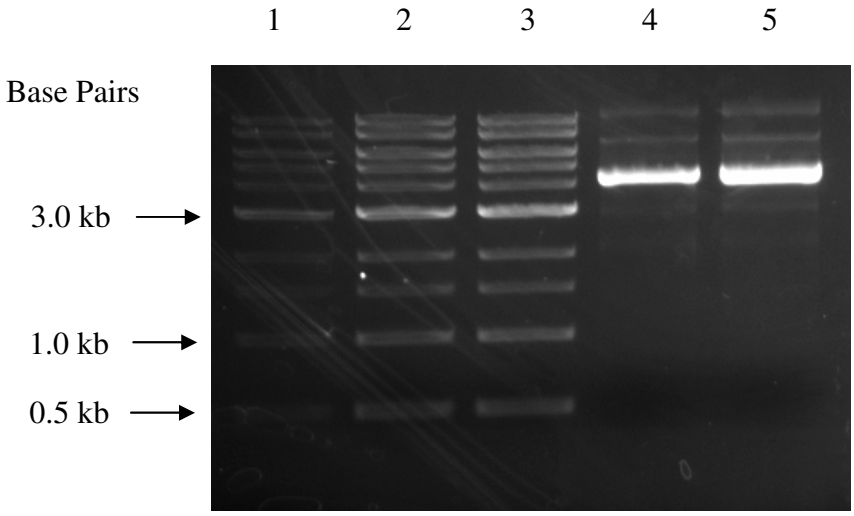

Figure 9. **Purified plasmid containing *S. enterica* BipA H527A substitution from two colonies.** An agarose gel showing DNA bands under UV light. Lanes 1, 2, and 3 contain a DNA ladder at concentrations of 0.5 µL, 1.0 µL, 2.0 µL, respectively. Lanes 4 and 5 contain a purified plasmid with the H527A substitution from two different colonies.

II. Expression and Purification

The pET28a plasmid was transformed into *E. coli* BL21 cells using heat shock and plated on kanamyacin plates. A single colony was taken from the plate to inoculate an overnight culture grown at 37°C. The overnight culture was diluted 1:20 into a day culture in LB nutrient broth and allowed to grow at 37° to mid log. 1.5 mL of culture was taken and labeled as "before induction" sample. Expression was induced with 1 M IPTG, diluted 1:1000 into the day culture. Culture was incubated at 37°C for 4 hours, cells harvested, and pellets resuspended in 30 mL of His-column binding buffer at pH 7.4 (20 mM HEPES pH 7.5, 50 mM NaCl, 20 mM Imidazole, 3 µM β-mercaptoethanol; adapted from GE Healthcare). Cells were sonicated for 3 x 30 seconds at 5.0 intensity and centrifuged in a SA600 rotor at 30,000 x g for 25 minutes at 14°C. Lysate was filtered through a 0.45 µm. The His-trap column was prepared by cleaning with 5 column volumes of water and binding buffer. Lysate was applied to the column, and purification

was completed with FPLC "His FF Crude" program. BipA substitution contructs were eluted with elution buffer at pH 7.4 (20 mM HEPES pH 7.5, 500 mM NaCl, 500 mM Imidazole, 3 μM β-mercaptoethanol, adapted from GE Healthcare).

III. Ribosome Binding Assay

The ribosome binding of each *S. enterica* BipA construct was examined using a continuous sucrose gradient. The plasmid pET28a was transformed into SB300 *Salmonella enterica* cells using electroporation, which were then plated on kanamyacin plates. A single colony was used to inoculate an overnight culture grown at 37°C. The overnight culture was diluted 1:20 into a day culture in LB nutrient broth and allowed to grow at 37° to mid log. BipA expression was induced with 0.2% Arabinose for 2 hours. The cells were harvested and resuspended in 1 mL of polymix buffer (5 mM $Mg(OAc)_2$, 0.5 mM $MgCl_2$, 5 mM NH_4Cl, 95 mM KCl, 8mM putrescine, 1mM spermadine, 5 mM KP_i, 1 mM dithioerythritol (DDT)) and sonicated at an intensity of 5.0 for 3 x 30 seconds (18). The lysate was clarified by centrifugation at 13,200 rpm and 4°C for 10 minutes.

Linear sucrose gradients were prepared from 7%, 17%, 27%, 37%, and 47% solutions. Seven mL of each sucrose solution was added to the bottom of a clear, thin-walled centrifuge tube, starting with the 7% solution. Each subsequent solution was added underneath the one before in order of increasing density. The tubes were sealed and allowed to linearize for 2-3 hours After adding a stopper to the tube, the gradients were placed on their sides to linearize for two to three hours.

Fifty OD_{254} units of the clarified lysate was placed on the top the of the sucrose gradient. The gradient was then centrifuged at 27,000 rpm and 13°C for 450 minutes in a

SW-28 rotor. The gradient was fractionated using a FPLC and monitored at 254 nm. Fractions corresponding to the 70S ribosome, 50S ribosome, 30S ribosome, and top of the gradient were pooled and precipitated with 10% trichloroacetic acid (Figure 10).

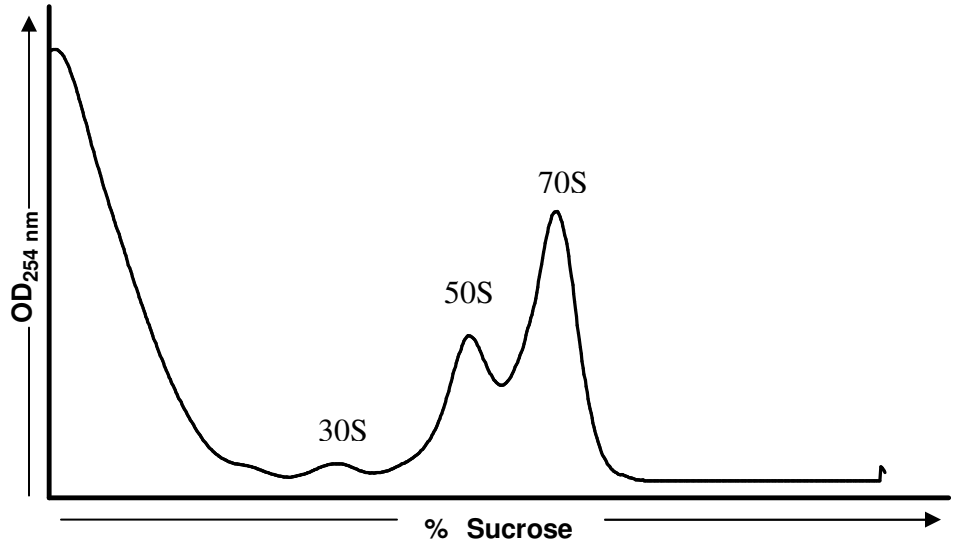

Figure 10**. Ribosome profile of BipA shows separation of 70S, 50S, and 30S species.** A profile obtained from fractionation of linear sucrose gradients by an AKTA-FPLC. The fractions corresponding to the 70S, 50S, 30S and top of the gradient were pooled and precipitated with trichloroacetic acid (Image courtesy of Dr. Victoria Robinson).

The samples were mixed thoroughly, incubated on ice for 15 minutes and centrifuged at 13,200 rpm and 4°C for 10 minutes). The supernatant was removed by pouring and 1 mL acetone was applied to the pellet without resuspension. The sample was centrifuged at 13,200 rpm and 4°C for 10 minutes. Acetone was carefully aspirated with a syringe, and the tubes were allowed to dry for 60 minutes. Samples were resuspended in 10x SDS sample buffer and separated on 12.5% SDS-PAGE. The gel was transferred onto PVDF membrane at 200 mA and 4°C for 960 minutes. The pET28a

vector introduces a N-terminal hexa-histidine tag to BipA, allowing the protein to be visualized using a HisDetector Western blot kit.

IV. Circular Dichroism (CD)

Circular dichroism reveals the secondary structural characteristics of proteins. This experiment was completed to ensure that site-directed substitutions that eliminated the 70S ribosome did not show significant disruption in secondary structure. BipA substitution constructs were expressed and purified as explained in section II, and dialyzed overnight with phosphate solution. Imidazole and other contaminants from the column interfere with the CD experiments by polarizing light while phosphate solution does not exhibit this activity. The concentration of the protein samples was determined by absorbance at 250 nm, and samples were diluted to 1 mg/mL in Circular Dichroism solution (20 mM phosphate, 150 mM NaCl). Since these experiments are sensitive to concentration, the absorbance wavescan was obtained again and the 1 mg/mL samples verified. CD experiments were completed using a cuvette path length of 0.1 mm and scans from 200 nm to 260 nm. Phosphate buffer was used to determine base-line values, which were auto-subtracted from the data.

V. Selection of Substitution Sites

Before ribosome binding assays could be used to determine the surfaces involved in the interaction between BipA and the ribosome, we had to determine which residues to substitute. Residues were chosen based on the an electrostatic model of BipA, the BindN program, which identifies potential RNA binding sites on proteins (19) and other

structural features of the C-terminal domain. The electrostatic map shows a large basic patch on the C-terminal domain of BipA. (Figure 11). Since RNA is a large component of the ribosome and the phosphate backbone of RNA is negatively charged, we hypothesized that residues located in this large, positively charged surface of BipA interact with the ribosome. Substitutions R507A and H527A were created to test this hypothesis.

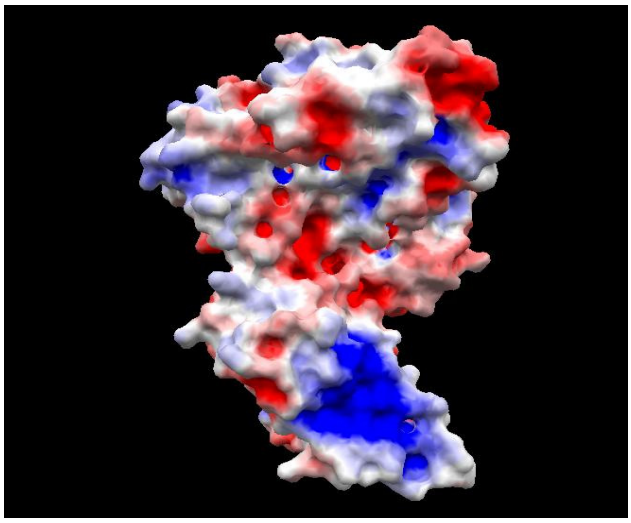

Figure 11. **Electrostatic map of BipA shows a basic patch on the C-terminal domain.** An electrostatic model of BipA. The C-terminal domain contains a large, basic patch that was targeted for site-directed mutagenesis. Residues R507 and H527 were selected as substitution sites to assess the contribution of this patch to ribosome binding (Image courtesy of Dr. Victoria Robinson).

The RNA binding prediction program, BindN, identified one region in domain IV and two regions in domain V as prime targets for site-directed mutagenesis. The prediction scheme identifies sites of potential contact with a red color and a confidence value (Figure 12). This value indicates the certainty with which the selected residue interacts with RNA, with a score of nine implying the highest certainty.

Figure 12. **RNA interaction sites predicted by BindN.** A analysis of the last three domains of the BipA sequence in the BindN program (17). The numbers to the left of each line correspond to the residue number of the leftmost amino acid in that line. The program identified one region in Domain IV (422-436) and two regions in Domain V (527-549 and 581-605) that are possible RNA interaction sites. Residues located in these three regions were selected for site-directed substitution.

In domain IV, residues 422 to 436 returned a positive prediction with confidence scores ranging from five to eight. Therefore, double substitutions of R422A/K423A and K434A/R436A were created to assess the ribosome binding properties of the region. In addition, the amino acid sequence from 527 to 549 in domain V represented a potential binding surface, with confidence values ranging from five to nine. In addition to its position on the C-terminal basic patch, H527 returned a positive prediction in this region. This helix, comprising of residues 597 to 607, is the third region that was deemed a potential binding surface according to the BindN prediction program.

In addition to data from the electrostatic map and RNA binding prediction program, other site-directed substitutions were created based on structural features of the C-terminal domain. R588 is believed to form a salt bridge with T315 from domain III and may be essential to stabilizing the relative positioning of domains III and V. Residue H514 lies very close to H527, and we were interested in determining whether the two residues could act interchangeably and overcome the loss of one histidine. Additionally, residues D532 and D552 flank a long, unstructured loop in the C-terminal domain, and substitutions were made at these locations to analyze the contribution of this structural element to ribosome association. We also probed K509 and K562 because these residues form a positively charged surface on a face adjacent to the large, basic patch in the C-terminal domain. Ribbon diagrams outlining the relative positions of the substitutions sites are shown in figure 13.

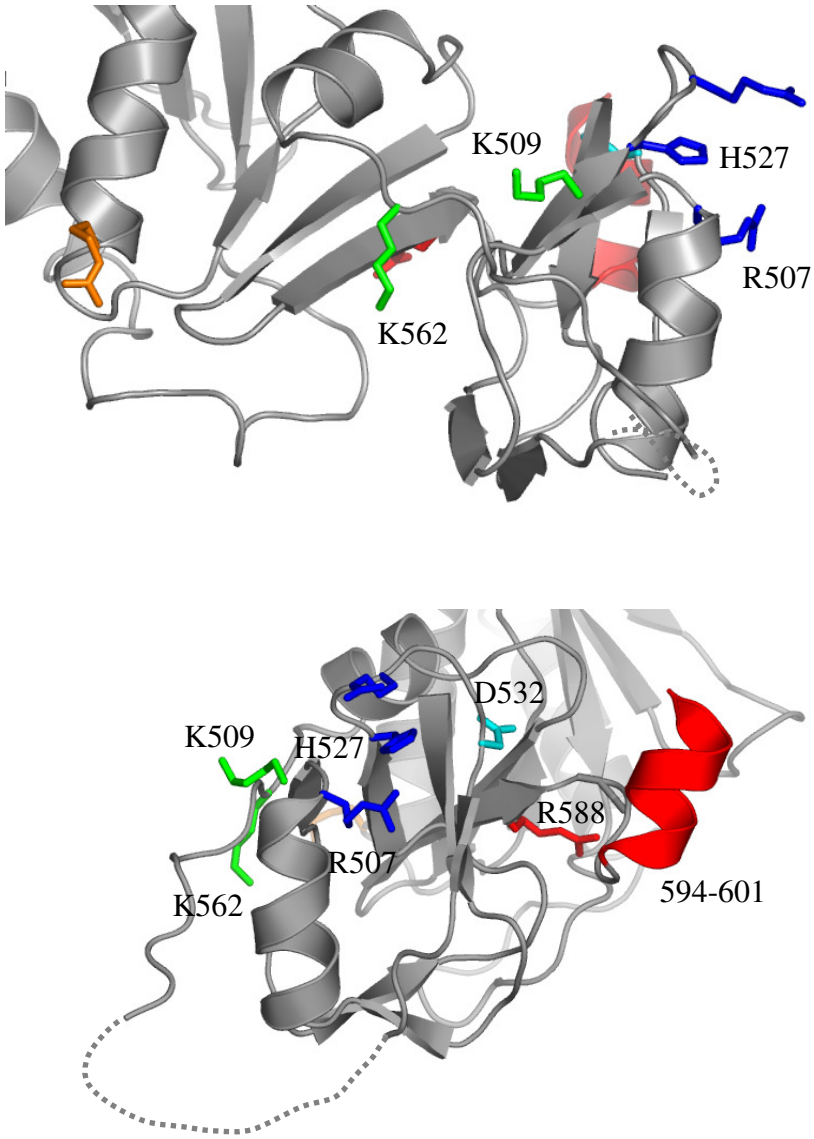

Figure 13. **Subsitution sites and truncated secondary structural elements in the BipA CTD.** A ribbon diagram showing the positions of residues substituted and structural elements removed in the experiments discussed in this thesis. Residues and structural features probed in these experiments are labeled and colored. R507 and H527 are part of a large, basic patch on the C-terminal domain. D532 is located within a large loop region in this domain. R588 forms a salt bridge with T315 (not visible) in domain III and lies very close to the C-terminal helix. K509 and K562 form a positively charged surface on a different face than the other basic patch. Residues 594-601 comprise the C-terminal helix that was removed in BipA (1-596). Residues that are not labeled reflect site-directed substitutions that are not discussed in this thesis (Images courtesy of Dr. Victoria Robinson).

Results

I. Domains III, IV, and V form the ribosome binding surface of BipA

As mentioned in the introduction, previous work in the Robinson lab revealed the C-terminal domain of BipA was necessary, but not sufficient for ribosome binding. Thus, we hypothesized that the 70S ribosome binding surface must extend beyond the C-terminal domain. A construct containing BipA domains IV-V also did not bind the 70S ribosome. However, the BipA III-IV construct investigated in this thesis co-fractionated with the 70S ribosome, suggesting that domains III, IV, and V form the ribosome binding surface of BipA (Figure 14).

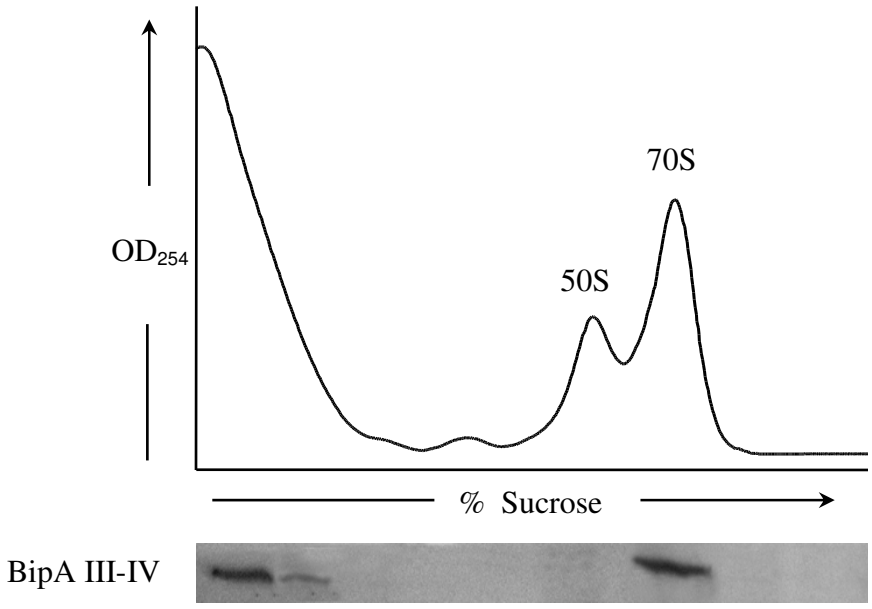

Figure 14. **BipA III-V construct co-fractionates with the 70S ribosome.** A Western blot showing ribosome binding for BipA III-IV. Sucrose density gradients were used to assess the ability of the N-terminal deletion construct to bind the ribosome.

II. The C-terminal helix is required for association with the 70S ribosome

Amino acid sequence analysis revealed that the last twenty residues of BipA are conserved across the family. Interestingly, the BindN RNA binding prediction program pinpointed residues 592-605 as potential interaction sites, with confidence values ranging from five to nine. This stretch of the protein has the strongest likelihood of binding RNA. Structurally, the residues at the C-terminal end form a basic helix, whose positive charges could potentially interact electrostatically with the negatively charged backbone of RNA. The BipA (1-596) deletion construct was created to investigate the contribution of this C-terminal helix to ribosome binding. Analysis by sucrose density centrifugation showed that BipA (1-596) pooled at the top of the gradient and did not bind the 70S ribosome (Figure 15).

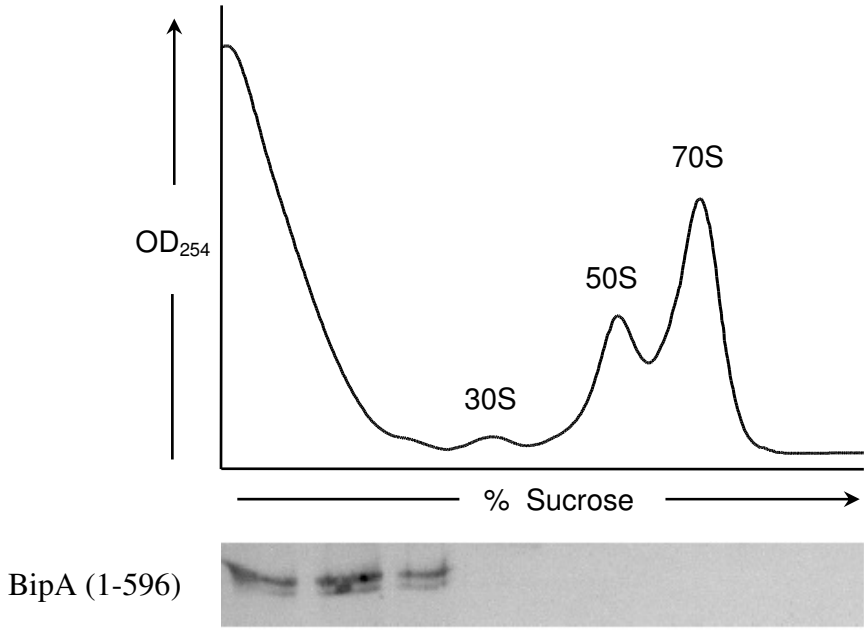

Figure 15. **BipA (1-596) does not co-fractionate with the 70S ribosome.** A Western Blot showing ribosome binding for BipA (1-596). Sucrose density gradients were used to assess the ability of the C-terminal deletion construct to bind the ribosome.

III. The 70S ribosome binding surface of BipA

The residues that were selected for site-directed mutagenesis using the electrostatic map, BindN program, and crystal structure were substituted with alanine using specially designed primers. Sucrose density gradients were then used to assess the ribosome binding ability of each substitution. Results of the ribosome binding experiments are shown in Figure 16. The K422A/R423A double substitution was able to bind the ribosome. K434A/R436A did not effectively bind the ribosome, but association was seen on the Western blot due to nonspecific interactions from overexpression of protein. Substitutions R507A, K509A, R507A/K509A, and K562A, did not alter BipA's ability to bind the ribosome. Construct H527A was not able to bind the ribosome, but further substitution with lysine at this site restored binding ability. Constructs D532A and D552A were able to complex with the ribosome independently, but the double substitution lost that ability. R588A, a substitution located at the interface between domains III and V, was not able to bind the ribosome.

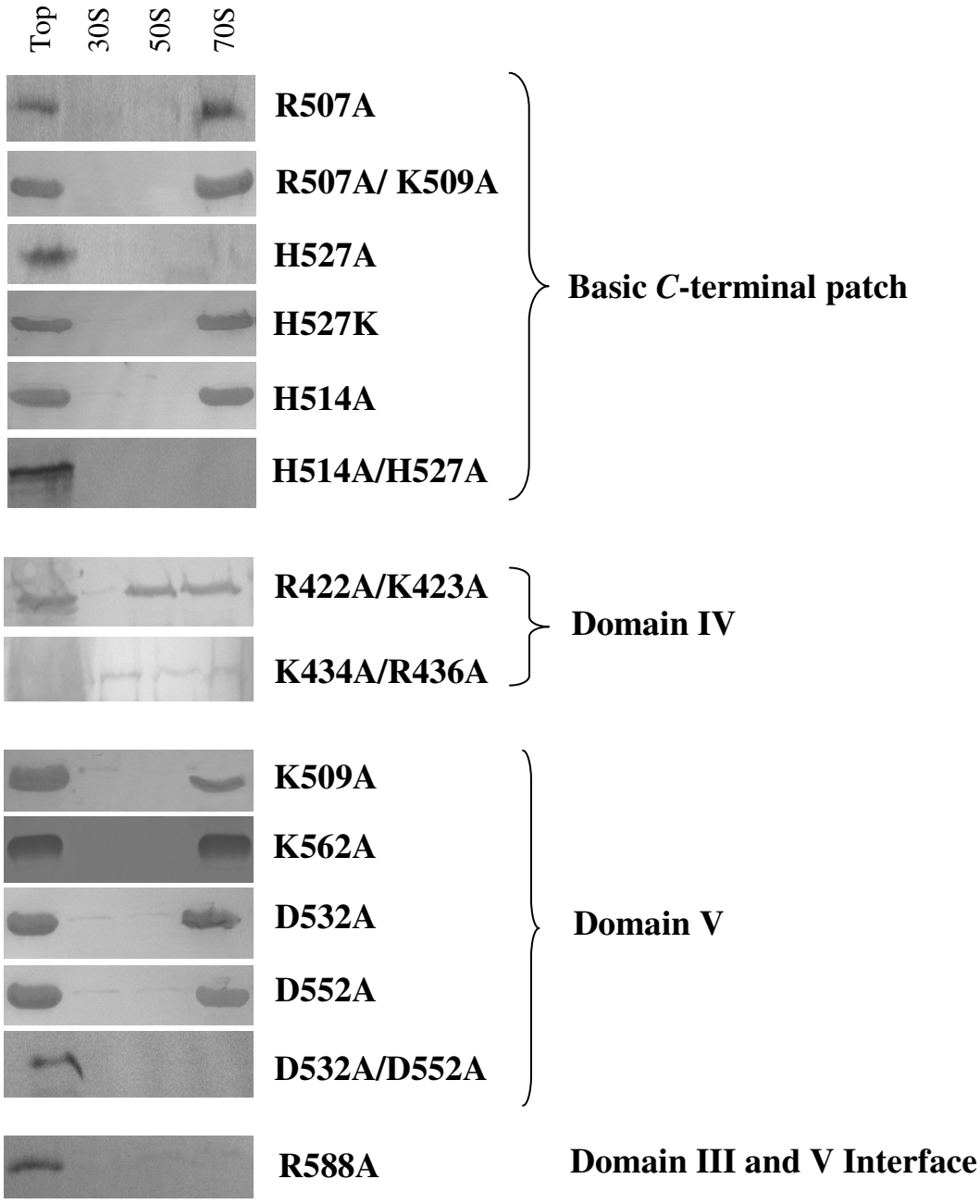

Figure 16. **Ribosome association assays for BipA site-directed substitutions.** Western blots showing ribosome binding of various BipA substitutions. Sucrose density gradients were used to assess binding ability of substitution constructs.

IV. Circular dichroism studies of BipA substitution constructs

Circular dichroism spectroscopy measures differential absorption in polarized light to determine secondary structural elements of proteins. We used CD to verify that loss of ribosome binding ability in BipA substitutions was due to a change in functionally important residues and not the result of significant structural disruption. Overnight dialysis in phosphate buffer was essential because even small remnants of the column elution buffer would alter the signal. H527A, H514A/H527A, and D532A/D552A gave spectra similar to that of wild-type BipA. In contrast, R588A showed a significant decrease in the spectroscopic signal, indicating a gross change in the secondary structure of the protein (Figure 17).

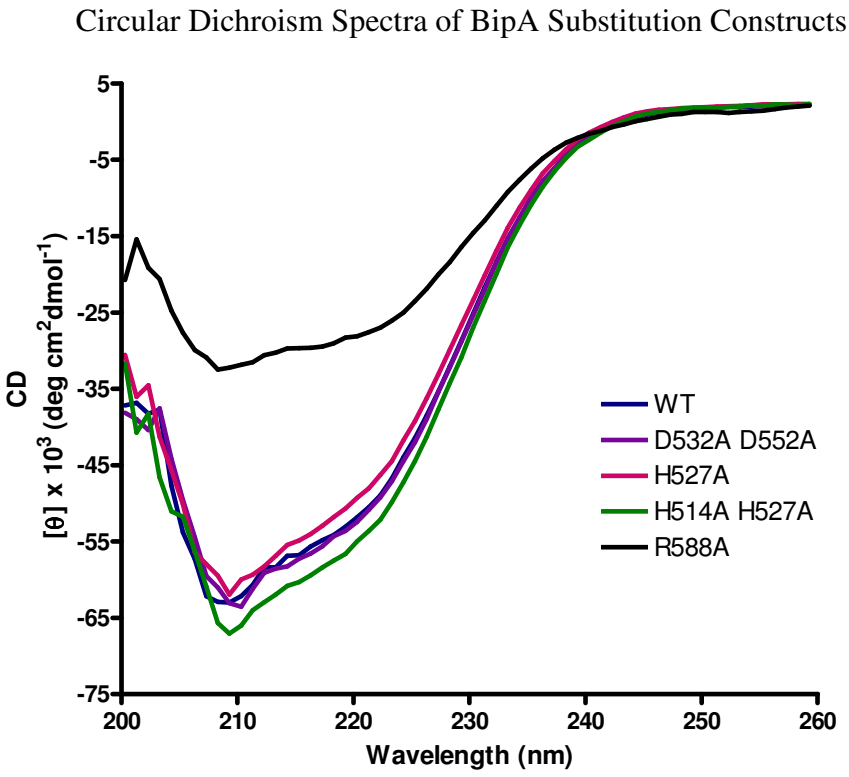

Figure 17. **Circular dichroism studies on BipA substitution constructs.** CD spectra of wild-type BipA and several substitution constructs. CD was used to detect disruption of secondary structure in substitution constructs as compared to wild-type BipA (Image courtesy of Dr. Megan deLivron).

Discussion

The GTPase BipA is a prokaryotic regulator essential to virulence and the stringent response. Conserved across many pathogenic species, BipA is a prime target for the development of antimicrobial agents. As mentioned earlier, BipA is a part of the translation family of GTPases, along with LepA and EF-G, whose members exert their cellular function through interactions with the ribosome. While the function of BipA remains unknown, previous data from the Robinson lab has shown that its novel C-terminal domain is essential to ribosome binding and that BipA associates with the ribosome in the GTP-bound state. However, an isolated BipA domain V construct was unable to bind the ribosome by itself, leading us to hypothesize that the ribosome binding determinants may extend beyond the C-terminal domain.

Structurally, BipA, LepA, and EF-G exhibit a great degree of similarity with the exception of the domain which is positioned distally to the G domain (domain V in BipA and LepA, domain IV in EF-G). We hypothesize that these domains impart structural specificity to each of these proteins, thereby promoting their differential binding to the ribosome. In support of this theory, Martemyanov et al. demonstrated that an EF-G protein missing domain IV was unable to bind the ribosome and support the translocation of tRNAs during protein synthesis (20). Therefore, investigation into the ribosome binding properties of BipA, in particular the participation of the C-terminal domain, was of great interest.

Data from the Robinson lab demonstrated that neither BipA domain V nor BipA IV-V were able to associate with the ribosome. As part of my work, sucrose density gradients were used to evaluate the ribosome binding affinity of BipA III-V. Data are

presented that this construct was able to bind the 70S ribosome, indicating that three C-terminal domains are sufficient for BipA to associate with the ribosome. However, this result does not necessarily indicate which structural elements of these domains are ribosome binding determinants. Considering the long loop regions and secondary structure interactions at the interfaces of BipA domains III, IV, and V, it is more likely that the presence of all three domains is required for proper spatial orientation of binding determinants. Therefore, we went on to probe distinct structural elements in this region of BipA in an attempt to identify the determinants that are required for ribosome association.

One of the elements that was investigated is a helix at the extreme C-terminal end of the protein. As mentioned earlier, the basic charge of the helix also makes it a prime candidate for electrostatic interactions with the negatively charged phosphate backbone of rRNA. Moreover, the crystal structure of EF-G domain IV displayed earlier in figure 6 also shows a long helix near the C-terminal end of the protein that directly contacts the 50S ribosomal subunit (21). The extreme C-terminal end of LepA has not been fully resolved. Sucrose density gradients showed that the basic helix is an essential ribosome binding determinant. These data are of greater significance because it supports previous evidence that showed that *E. coli* with a truncated BipA protein (loss of eleven C-terminal amino acids) lose the ability to colonize mouse large intestine (22). In tandem, both data support that ribosome binding and function are related in BipA, a relationship that is true of all members of the translational GTPase family.

Protein-protein and protein-nucleic acid interactions are governed by the surface properties of the elements involved. Alanine scanning was used to chart the 70S ribosome

binding surface of BipA. An electrostatic map of BipA showed a large, basic patch on the C-terminal domain, which was implicated as a site of possible electrostatic interactions with rRNA. However, substitution R507A was not able to eliminate ribosome binding. The H527A construct was unable to bind the ribosome, but its binding ability was restored in the construct H527K. This result suggests that a positive charge at residue 527, perhaps to interact with a negatively charged surface on the ribosome, is essential to binding. Interestingly, residue 527 in EF-G is essential for translocation (20). In related experiments in the Robinson lab, it was demonstrated that residue H529, also in this patch and identified as a potential contact site by BindN, is a ribosome binding determinant. The crystal structure shows that H527 sits directly in the middle of the basic patch, while H529 lies above it and R507 lies below it. The data suggest that integrity of the upper region of the basic patch is essential to ribosome association.

The BindN RNA binding prediction program identified three areas in domain IV and V as potential RNA interaction sites. Substitutions R422A/K423 and K434/R436A were created to probe a small region in domain IV, and these substitutions were able to bind the ribosome. However, it does not appear that K434A/R436A is able to bind effectively, as high expression of the construct led to minimal co-fractionation with ribosomal species. H514 was probed to see whether a residue in close proximity to H527, a potential binding site identified by the BindN program, showed similar importance in ribosome associations. However, H514A bound the 70S ribosome, eliminating this residue as a potential contact site. The third region of RNA binding from the prediction program was the C-terminal helix that was discussed earlier in this section.

The final criteria for determining amino acid sites for alanine scanning involved examining the structural features of the C-terminal domain. D532 and D552 flank a long loop region in the CTD. Interestingly, single substitutions at sites 532 and 552 did not alter ribosome binding, but the double substitution D532A/D552A was not able to associate with the ribosome. Both K509A and K562A co-fractionated with the 70S ribosome, implying that the secondary positively charged surface in the C-terminal domain was not involved in binding. R588A was also unable to bind the ribosome. As mentioned earlier, this residue forms a salt bridge with an T315 in domain III that may be essential to the preservation of the C-terminal helix. The CD spectra of R588A shows a decrease in signal at 210 nm, which is consistent with loss of α-helical secondary structure. Again, we observe that elements of domain III have an effect on the ribosome binding determinants in other domains.

Circular dichroism was used to analyze secondary structural features of those substitutions that did not associate with the ribosome. We wanted to ensure that loss of binding was due to a change in a functionally important residue and not in the gross structure of BipA. H514A/H527A, H527A, and D532A/D552a gave spectra characteristic of wild-type BipA, indicating that these substitutions were indeed altering residues essential to ribosome binding.

Figure 18 outlines a map of the ribosome binding determinants and switch regions of BipA. In the C-terminal domain, two distinct areas that lie in close proximity are involved in ribosome association. Residues in other domains that influence binding also lie on the same side of BipA, suggesting that one face makes direct contact with ribosomal elements. The switch regions lie on the opposite face of BipA.

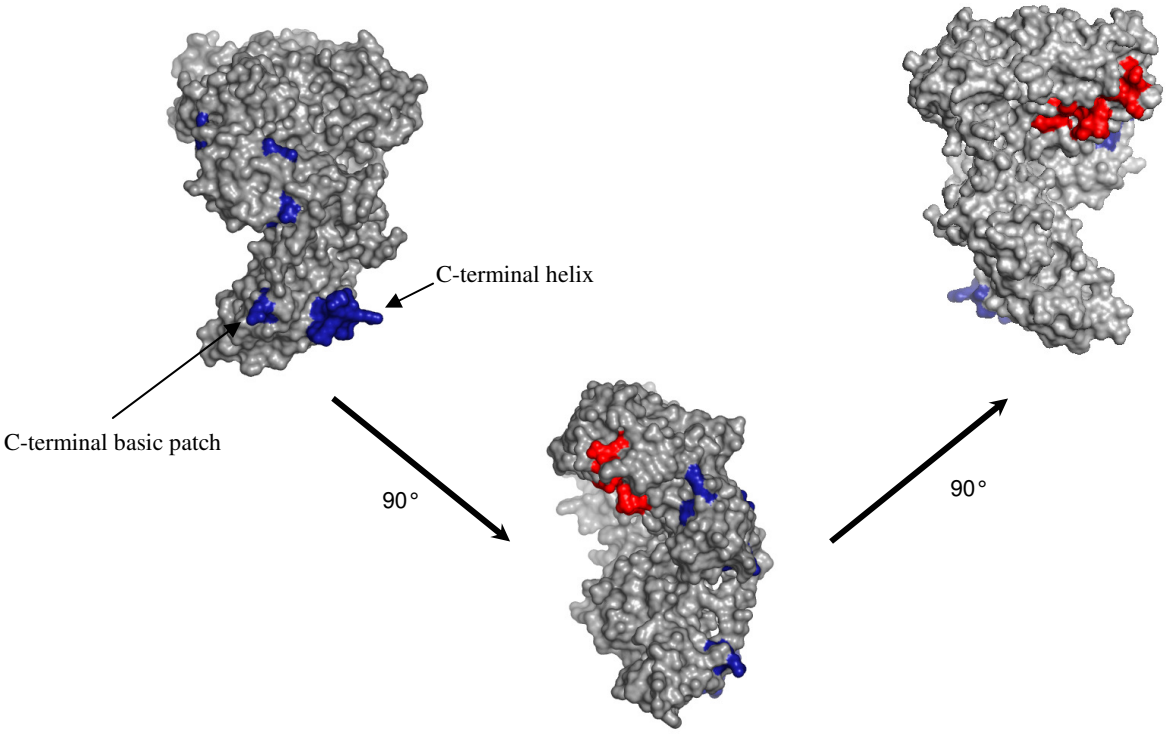

Figure 18. **A model of the BipA ribosome binding determinants and switch regions.** A space-filling model of BipA highlighting regions implicated in ribosome association. The blue areas of BipA represent surfaces that are involved in ribosome binding, and the red areas represent the switch regions of the protein (Image courtesy of Dr. Victoria Robinson).

Data from the Robinson lab has also shown that BipA associates with the 70S ribosome in the GTP-bound state. Characteristic of the mechanism of G protein switching, we hypothesize that GTP binding alters the surface properties of BipA, increasing its affinity for the ribosome. The "on" state can only be achieved by proper contact with the ribosome, which in turn can only be achieved by GTP binding. It is yet to be investigated whether nucleotide binding may be altering other surface areas on BipA that may be directly related to its cellular function. It is also plausible that direct contact with the 70S ribosome could change the conformation of BipA and play a role in designating the protein's function. More experiments are needed to support these hypotheses.

In conclusion, the work explained in this thesis supports the novel C-terminal domain of BipA as an essential feature for ribosome association. In fact, domains III, IV, and V are necessary for complex formation. Akin to other members of the translation family of GTPases, BipA exerts its cellular function through interactions with the ribosome. This preliminary analysis of ribosome binding properties may prove essential to revealing the function of BipA and eventually designing new antimicrobials to combat the ever-growing threat of resistant bacterial species.

References

1. Caldon, C.E., Yoong, P., and March, P.E. (2001) *Evolution of a molecular switch: universal bacterial GTPases regulate ribosome function.* Mol Microbiol 2: 289–297.

2. Vetter, I. R. and Wittinghofer, A. (2001). *The guanine nucleotide-binding switch in three dimensions.* Science 294, 1299-1304.

3. Bourne, H.R., Sanders, D.A., and McCormick, F. (1991) *The GTPase superfamily: conserved structure and molecular mechanism.* Nature 349: 117–127.

4. Yonath A. (2005) *Antibiotics targeting ribosomes: Resistance, selectivity, synergism, and cellular regulation.* Annu. Rev. Biochem**.** 74: 649–679.

5. Wilson, D. N., and Nierhaus K.H**.** (2003). *The ribosome through the looking glass.* Angew. Chem. Int. Ed. Engl. 42**:**3464-3486.

6. Davidson, Michael. "Ribosomes." Molecular Expressions Cell Biology. 4 Jan. 2005. Florida State University

7. Qi, S.Y., Li, Y., Szyroki, A., Giles, I.G., Moir, A. and O'Connor C.D. (1995) *Salmonella Typhimurium responses to a bactericidal protein from human neutrophils.* Molecular Microbiology 17, 523–531.

8. Farris, M., Grant, A.A., Richardson, T.B., and O'Connor, C.D. (1998) *BipA: a tyrosine-phosphorylated GTPase that mediates interactions between enteropathogenic Escherichia coli (EPEC) and epithelial cells.* Mol Microbiol 28**:** 265–279.

9. Grant, A.J., Farris, M., Alefounder, P., Williams, P.H., Woodward, M.J., and O'Connor C.D. (2003) *Co-ordination of pathogenicity island expression by the BipA GTPase in enteropathogenic E. coli (EPEC).* Molecular Microbiology. 48(2): p.507-521.

10. deLivron, M.A., Robinson, V.L. (2008) *Salmonella enterica Serovar Typhimurium BipA Exhibits Two Distinct Ribosome Binding Modes.* J. Bacteriol. 190: 5944-5952.

11. Pfennig, P.L., Flower, A.M. (2001) *BipA is required for growth of Escherichia coi K12 at low temperature*. Mol Genet Genomics 266:313–317.

12. Krishnan, K., Flower A.M. (2008) *Suppression of {Delta}bipA Phenotypes in Escherichia coli by Abolishment of Pseudouridylation at Specific Sites on the 23S rRNA.* J. Bacteriol. 190: 7675-7683.

13. Agrawal, R.K., Penczek, P., Grassucci, R.A., and Frank, J. (1998) *Visualization of elongation factor G on the Escherichia coli 70S ribosome: The mechanism of translocation.* Proc. Natl. Acad. Sci. 95: 6134–6138.

14. Qin, Y., Polacek, N., Vesper, O., Staub, E., Einfeldt, E.,Wilson, D. N. & Nierhaus, K. H. (2006). *The highly conserved LepA is a ribosomal elongation factor that back-translocates the ribosome.* Cell, 127, 721–733.

15. Evans, R.N., Blaha G., Bailey, S., Steitz, T.A. (2008). *The structure of LepA, the ribosomal back translocase.* PNAS 105: 4673-4678.

16. Joergensen, R., Ortiz, P.A., Carr-Schmid, A., Nissen, P., Kinzy, T.G., Andersen, G.R. (2003) *Two crystal structures demonstrate large conformational changes in the eukaryotic ribosomal translocase*. Nat.Struct.Mol.Biol. 10**:** 379-385.

17. Zheng, L., Baumann, U., and Reymond, B.L.**.** **(**2004). *An efficient one-step site-directed and site-saturation mutagenesis protocol*. Nucleic Acids Res. 32:e115.

18. Abdulkarim, F., Ehrenberg, M., Hughes, D. (1996). *Mutants of Ef-Tu defective in binding aminoacyl-tRNA*. FEBS Lett. 382:297–303.

19. Wang, L., and Brown, S.J. (2006) *BindN: a web-based tool for efficient prediction of DNA and RNA binding sites in amino acid sequences*. Nucleic Acids Res., 34, W243–W248.

20. Martemyanov, K.A. and Gudkov, A.T. (1999) *Domain IV of elongation factor G from Thermus thermophilus is strictly required for translocation.* FEBS Lett. 452, 155–159.

21. Agrawal, R.K., Penczek, P., Grassucci, R.A. and Frank, J. (1998) *Visualization of elongation factor G on the Escherichia coli 70S ribosome: the mechanism of translocation.* Proc. Natl Acad. Sci. USA, 95, 6134–6138.

22. Moller, A. K., Leatham, M.P., Conway, T., Nuijten, P.J., de Haan, L.A.M., Krogfelt, K.A., and Cohen, P.S. (2003). *An Escherichia coli MG1655 lipopolysaccharide deep-rough core mutant grows and survives in mouse cecal mucus but fails to colonize the mouse large intestine*. Infect. Immun. 71: 2142–2152.